Chiang Mai J. Sci. 2020; 47(4) : 838-853
http://epg.science.cmu.ac.th/ejournal/
Contributed Paper

Dry Sliding Wear Behavior of Sintered SS316L-Sn Containing MoS_2 Solid Lubricant

Wantana Koetniyom [a,b], Yossawas Nopjinda [a], Romechalee Tepnok [a], Nattaya Tosangthum [c], Monnapas Morakotjinda [c], Thanyaporn Yotkaew [c], Pongsak Wila [c] and Ruangdaj Tongsri*[c]

[a] Department of Industrial Physics and Medical Instrumentation (IMI), Faculty of Applied Science, King Mongkut University of Technology North Bangkok, Bangkok 10800, Thailand.

[b] Lasers and Optics Research Center (Landos), King Mongkut University of Technology North Bangkok, Bangkok 10800, Thailand.

[c] Particulate Materials Processing Technology Laboratory (PMPT), Metal and Manufacturing Process Research Group (MMP), National Metal and Materials Technology Center,114 Paholyothin Road, Khlong Nueng, Khlong Luang, Pathum Thani 12120, Thailand.

*Author for correspondence; e-mail: ruangdt@mtec.or.th

Received: 25 July 2019
Revised: 23 December 2019
Accepted: 10 February 2020

ABSTRACT

Traditional powder metallurgical process is commonly used for producing self-lubricating composites. Solid lubricant dispersion in the steel matrices affects tribological properties by lowering friction coefficient leading to lifetime extension of steel matrix composite parts. Molybdenum disulfide (MoS_2) is one of the most used solid lubricants since its lamellar crystalline structure can form a sliding film adhering to the rubbing surfaces. The sliding film acts as anti-friction or anti-wear layer. Due to such action, MoS_2 is widely used for providing friction reduction in a situation where the use of liquid lubricants is impractical. However, MoS_2 decomposes and reacts with the matrix at high temperatures, usually employed for producing sintered self-lubricating composites. The reaction leads to undesirable products when the powder metallurgical route is used to incorporate MoS_2 into steel matrices. In order to lessen undesirable reaction, the temperature-activated phenomenon, resulting in decrease of lubricating efficiency, it is necessary to find the method for mitigating decomposition and reaction. In this work, tin (Sn) powder was added to the mixtures of 316L stainless steel and MoS_2 powders with expectation that sintering enhancement by Sn powder addition would reduce sintering temperatures and thus reduce MoS_2 + 316L reaction. Varied MoS_2 contents (5, 10 and 15 wt. %) were mixed with fixed 4 wt. % Sn and balance 316L stainless steel powder. The green compacts of powder mixtures were sintered at temperatures of 1,150 $^{\circ}$C and 1,200 $^{\circ}$C in hydrogen atmosphere for 45 min. Mechanical properties and dry-sliding wear behavior of the sintered composites were investigated. Liquid phase sintering due to Sn powder addition was observed. However, the energy dispersive spectroscopy (element mapping mode) showed that the reaction between MoS_2 and alloying elements in 316L powder occurred and resulted in sulfide formation. It was found that the amount of added MoS_2 had influences on the tensile properties, hardness and sintered density. Although wear resistance and friction coefficient slightly increased according to the MoS_2 content, the added MoS_2 amounts higher than 10 wt.% led to adverse effect.

Keywords: powder metallurgy, solid lubricants, molybdenum disulfide, friction coefficient

1. INTRODUCTION

Nowadays, the increasing demand for higher performance engineering materials in severe operating conditions is a driving force for the development of new materials. Indicators for higher performance materials development are efficiency, safety, energy consumption and environment-friendly. The trend of applications of solid lubrications for expanding service lifetime of materials shows rapid increase in the past few decades. Solid lubrications have become highly attractive substitutes for liquid lubricants, such as hydraulic oils and semisolid lubricants, such as greases since they are environmentally friendly and less toxic. They can be applied to components of a tribological pair in the forms of either dispersed particles or surface films in the condition that the use of liquid lubricants is impractical such as under high vacuum, cryogenic temperatures and radiation environments [1]. Molybdenum disulfide (MoS_2) is one of the most used solid lubricants. Low friction property is related to its crystal structure which has strong chemical bonds within the plane and weak interactions between the planes like graphite. However, its performance decreases in the presence of humidity which can deteriorate lubricating ability by oxidation [2].

Powder metallurgical (PM) process commonly used for producing self-lubricating composites of which the production cost is close to that for the similar parts without solid lubricant. To obtain a composite with a good compromise between high mechanical properties and a low friction coefficient, it is necessary that the composite matrix has a high degree of bonding, the solid lubricant added is not soluble and does not react with the matrix otherwise the solid lubricant may loss its lubricant characteristic. The examples of metals used in the self-lubricating composites are copper based, iron based and nickel based materials. Copper-based composites are used for thermal management application due to excellent thermal conductivity property [3]. However, they have low mechanical resistance and narrow range of application temperatures. Iron based self-lubricating composites are vastly increased over copper-based ones, due to their higher mechanical properties. Application of such composites include automotive such as piston ring, clutch, brake system and engine liners [4].

Stainless steels have excellent corrosion resistance but poor tribological properties, which can be improve by the additions of solid lubricants [5]. It has been known that 316L stainless steel containing a solid lubricant produced by PM techniques might be appropriate for reducing friction and preventing welding under conditions of metal contact pairs [6-8]. Stainless steels are usually used for automotive, electrical and electronic applications. It has been reported that reactions between the matrix and solid lubricants resulting in modification of tribological characteristics of composites produced from stainless steel (18%Cr-15%Ni) mixed with Cr_3C_2 (10 to 30 wt.%) and MoS_2 (2 to 8 wt.%) [9]. Cr_3C_2 reacted with the matrix at temperature above 1,220 °C whereas MoS_2 already reacted at low temperature of around 800 °C. These reactions can change the microstructure and mechanical property resulted from the presence of islands of pearlite, complex carbides and sulfides in the austenitic matrix due to the diffusion of alloying elements such as Cr, C and Mo into the matrix. Thereby, the composites presented high friction coefficients but lower wear rate. Slys et al. [10] also reported about reaction between the solid lubricant and the matrix of sintered composites produced from stainless steel (23%Cr-18%Ni) mixed with 10 to 50 wt. % of MoS_2. The microstructure of samples revealed the sulfides of both Fe and of Cr plus a eutectic phase dispersed in stainless steel matrix. XRD analysis confirmed that the absence of MoS_2 phase meanwhile $Fe_{1-x}S$, $Cr_{0.83-0.87}S$, Fe_3Mo and FeCrMo phase were presented.

Mahathanabodee et al. [11] prepared sintered composites of AISI 316L containing MoS_2 and h-BN (10 to 20 vol. %). Dry sliding wear test was carried out using a pin-on-disc tribometer (ASTM

G99) under sliding speed of 0.1 and 0.2 m/s with load of 3 N. The study results indicated that the density, hardness and wear resistance decreased with increasing h-BN content but increased with increasing MoS_2 content. The addition of h-BN to stainless steel showed lubricating characteristic better than that of MoS_2. Worn surfaces of the sintered SS316L/MoS_2 examined by using SEM revealed that wear mechanism dominated by adhesive and delamination.

Raadnui et al. [12] reported the mechanical and tribological behavior of sintered 316L stainless steel incorporated with MoS_2. Specimens were sintered at 1300 ºC for 45 min under hydrogen atmosphere. Wear testing was performed by using a partial plain bearing wear test rig with the PV values between 1.1 and 1.8MPa m/s. It was found that the density and tensile properties of the specimens decreased as the amount of MoS_2 increased. On the other hand, the hardness increased with increasing MoS_2 content. MoS_2 was actually beneficial in reducing the friction and wear of the composites. Especially, the sintered 316L+15wt. % MoS_2 material at 1.1 PV exhibited a diminution of friction coefficient when compared to the sintered 316L specimen without MoS_2 addition. Moreover, they found that, weight loss increased with increasing of MoS_2 content when too high load was employed. This was due to a low shear strength of sintered composites.

Furlan et al. [13] reported the effect of addition of alloying elements (P, Mo and Cr) on retarding the reaction between the iron matrix and MoS_2 solid lubricant, due to an alternation in the chemical potential of the matrix. Reaction products were iron sulfides/chromium sulfides and iron molybdenum mixed sulfides that vary according to the sintering temperature. It was found that for a sintering temperature of 1,150 ºC, chromium iron mixed sulfide had more stable than the iron sulfide. This result conforms to those published in other papers [14-16]. The reaction with stainless steel sample (SS316L) containing basically Cr, Ni, Mo and Si produced chromium sulfide, which was also found in the reaction with 17-4 PH [17]. Tribological properties of samples with additions of alloying elements (P, Mo and Cr) using ball on disc reciprocating test were also reported. The iron molybdenum mixed sulfides and the chromium sulfide did not show equally good lubrication properties as MoS_2 did.

Sn powder has previously been used as a liquid phase sintering aid that lowers the sintering temperature of SS316L [18]. It is also used as a solid lubricant because it is a soft metal having multiple slip planes in the crystal structure and it does not undergo work-harden during sliding [19]. In this work, Sn powder was added to the mixtures of 316L and MoS_2 powders with expectation that its sintering enhancement would reduce sintering temperatures and thus reduce MoS_2 + 316L reaction. The improved lubricating property of the sintered 316L+MoS_2+Sn composites was aimed at in this work.

2. MATERIALS AND METHODS

2.1 Materials

The concept of this work is using low sintering temperature to produce self-lubricating composites containing MoS_2 in order to avoid the dissociation of MoS_2 due to reaction with 316L stainless steel matrix. In this work, Sn powder was used as a liquid forming powder for enhancing sinterability of SS316L + MoS_2 composites. The influence of varied weight percentages of MoS_2 on the mechanical and lubricating properties were investigated. The base powder of this experiment is stainless steel powder grade AISI316L which is produced by gas atomization and is supplied by Hoganas Company of Sweden. Sn powder was produced by using gas atomization. Details of the gas atomizer set up are given in [20]. MoS_2 powder is supplied by Climax Molybdenum, Phoenix AZ, USA). Particle size of 316L stainless steel powder, and MoS_2 powder were in the range of 25-75 μm, and 11-25 μm respectively. Sn powder particles were sieved to less than 32 μm. SEM micrographs and EDS analysis of (a) 316L, (b) MoS_2 and (c)

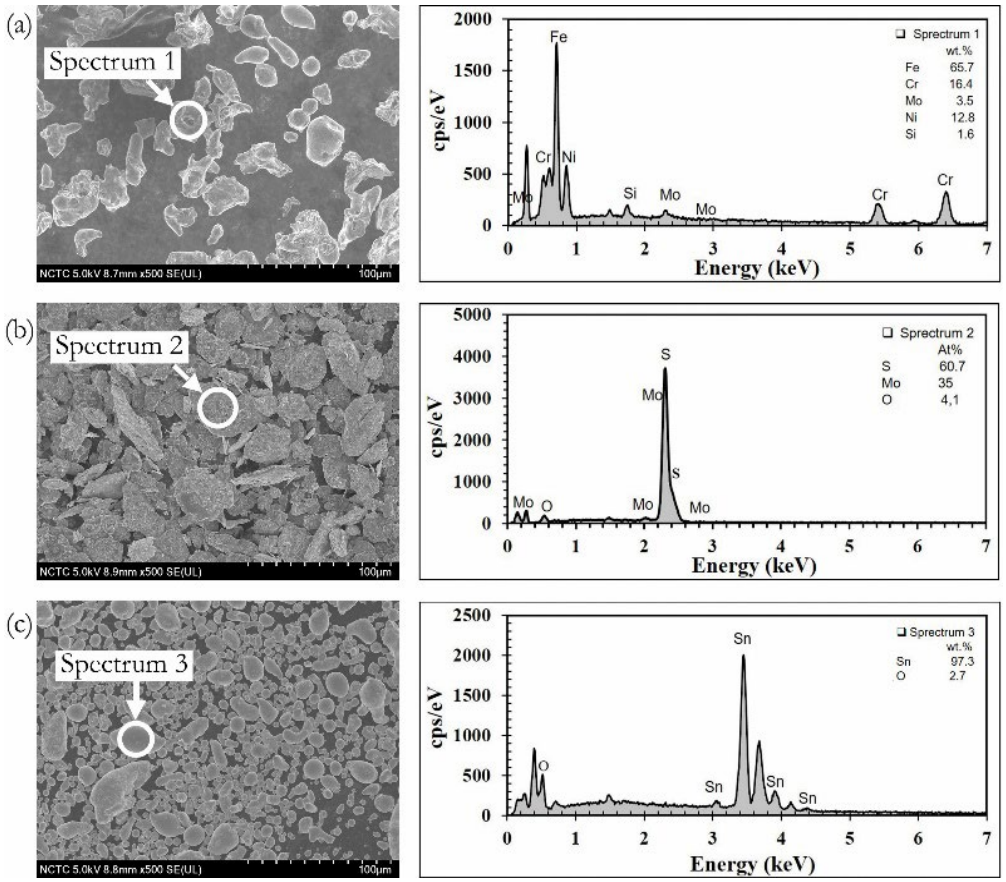

Figure 1. SEM micrographs and EDS analysis of SS316L (a), MoS_2 (b) and Sn powders (c).

Sn powders are shown in Figure 1.

2.2 Specimen Preparation

The specimens were designed to contain varied contents of MoS_2 powder. Four sets of specimens included (1) 316L+ 4wt.%Sn without MoS_2, (2) 316L+4 wt.%Sn+5 wt.% MoS_2, (3) 316L+4 wt.%Sn+10 wt.% MoS_2, and (4) 316L+ 4wt.%Sn +15wt.% MoS_2. The 1.0 wt. % of zinc stearate was added to act as a pressing lubricant. Mixing of each specimen set was performed in a barrel mixer rotating with the speed of 10 rpm for 30 min. After that, the admixed powders were compacted into standard tensile test bar according to MPIF standard 10, ASTM B783 and also compacted into disc specimens with dimensions of 30 mm diameter and 5 mm thick by using a uniaxial pressing machine (DORST). Densities of the green compacts were 6.5 ± 0.05 g/cm^3. The densities of the green and sintered samples were determined using Archimedes method as given in MPIF Standard 42. The green compacts were heated at 5 ºC/min to 600°C and held for 30 min to remove zinc stearate in argon. Then the green compacts were heated at 5 ºC/min to sintering temperatures of 1,150 ºC and 1,200 ºC under hydrogen atmosphere (the flow rate of 200 L/h) for 45 min. The sintered specimens were cooled down in the furnace with the rate of 0.1°C/s. The microstructures of sintered samples were observed by optical microscopy (OM) and scanning electron microscopy (FESEM-HITA-

CHI/SU8230). Chemical analysis was conducted by using energy dispersive X-ray spectroscopy (EDS). Hardness of the sintered specimens was carried out using a hardness tester (Rockwell scale B). Tensile properties were tested by using Universal testing machine (Instron 8801).

2.3 Wear Test

In this work, pin-on-disc wear testing machine was used to investigate the sliding behavior and relevant wear mechanism of the sample materials under dry condition. The tests were performed using an applied load of 10N with sliding speed of 0.2 m/s, track radius of 60 mm and the total sliding distance of 1000 m. During the test, a steel ball (hardness of 65HRC) with diameter of 6 mm was pressed against the rotating disc sample. The friction coefficient was determined during the test by direct measurement of the change in torque by a sensor. Weight loss of each specimen after thorough cleaning with acetone solution was obtained by weighing the specimen before and after the experiment by a digital balance having an accuracy of ±0.001 g. SEM was used to investigate the morphology of the worn surface of specimens after wear tests.

3. Results and Discussion

3.1 Microstructures

The microstructures of sintered 316L + Sn + MoS_2 composites, produced by sintering at 1150 and 1200 ºC for 45 min under hydrogen atmosphere, were observed by OM as shown in Figure 2.

It was found that the addition of 4 wt. % Sn could facilitate sintering of 316L + Sn and 316L + Sn + MoS_2 powder compacts. At the sintering temperature of as low as 1150 °C, the microstructures of sintered 316L + Sn and 316L+Sn+ MoS_2 composites showed sintered bonds as results of both solid-state and liquid-phase sintering (LPS). In the sintered 316L+Sn+MoS_2 composites, there were dark spots distributed within 316L matrix. The increase of sintering temperature to 1200 °C slightly affected the microstructures of sintered composites in terms of microstructural component and size. The dominant microstructural feature of the sintered 316L+Sn+ MoS_2 composites was the thick intergranular phases, which represented the products of reaction occurring during heating and sintering. The volume fraction of thick intergranular phases increased with increasing MoS_2 content and slightly increased with increasing sintering temperature.

The shape of thick intergranular phases indicates that they are the solidified products of liquid phase formed during heating and sintering. The formation of liquid phase could be due to Sn powder melting [18, 21, 22] and the reaction between 316L powder constituents with MoS_2 [9, 10, 12]. The secondary electron images, given in Figure 3, show contrast between different intergranular phases including dark and bright intergranular phases. In addition to the intergranular phases, dark spots were observed inside 316L matrix. For each sintering temperature, the number of dark spots increased with increasing MoS_2 content. When the sintering temperature was increased to 1200 °C, the number of dark spots was slightly decreased. On the other hand, the 316L matrix was cleaner when the composites were prepared at a higher temperature. It was previously reported that sulfide particles were formed in the middle of iron particles in sintered Fe + MoS_2 composites [23]. The formation of sulfide particles in the middle of Fe particles was due to the diffusion of S into Fe matrix and the excessive S concentration above its solid solubility in Fe led to iron sulfide formation.

Regarding grain growth associated with LPS, the increase of sintering temperature from 1150 to 1200 °C did not promote grain growth in sintered 316L + Sn and 316L+Sn+ MoS_2 composites. The grain growth was observed 316L + Sn alloys sintered at 1300 °C [21, 22]. The grain growth suppression may be due to low sintering temperature and grain boundary movement hindered by thick intergranular phase.

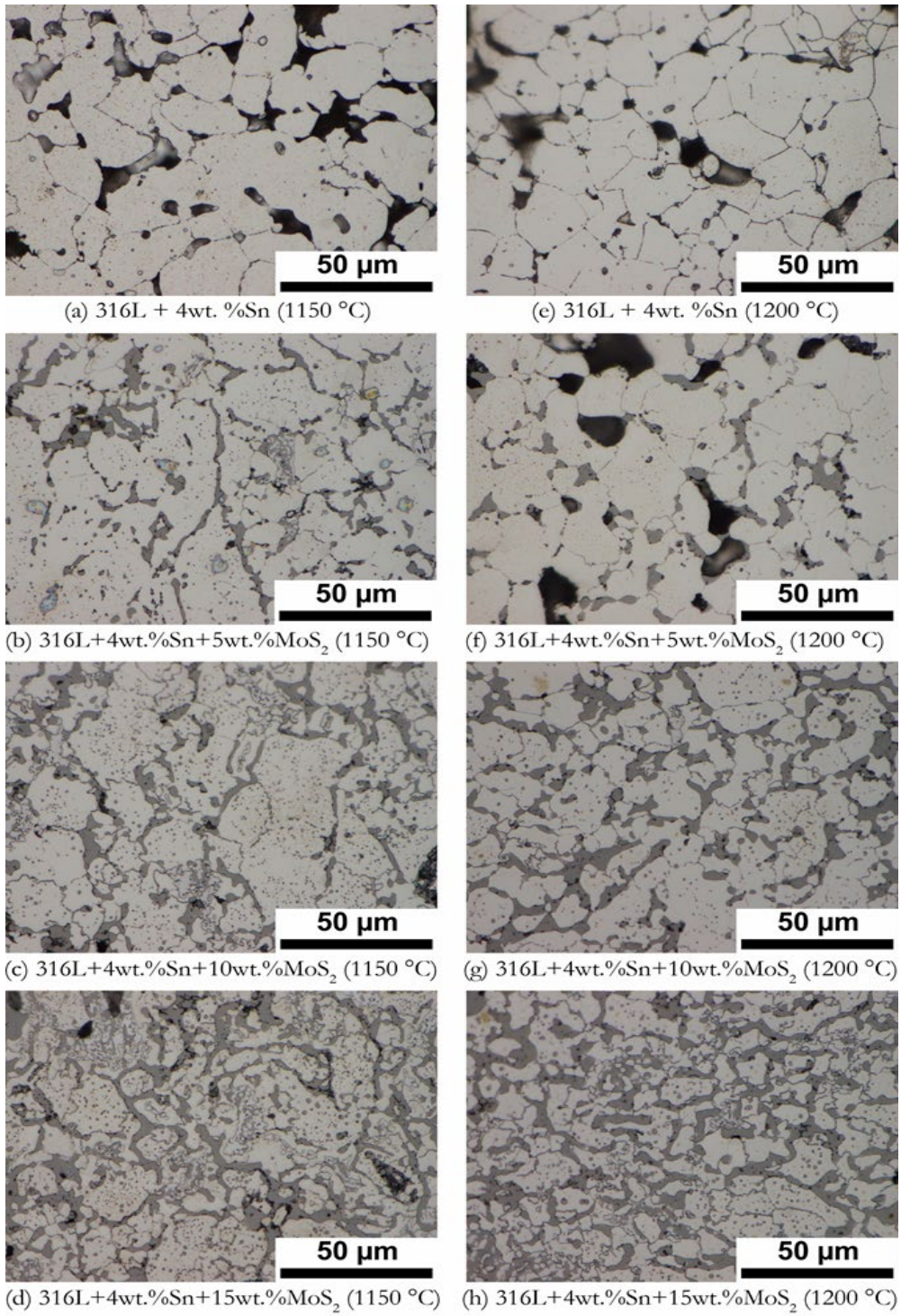

Figure 2. Optical images of SS316L composites containing 4 wt.%Sn with variation in MoS_2 addition sintered at 1150 ºC (a, b, c, d) and 1200ºC (e, f, g, h).

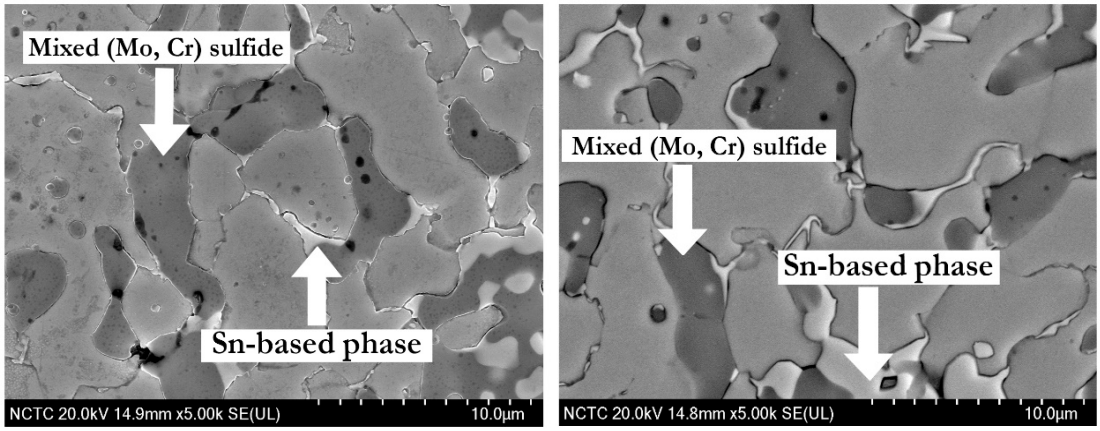

Figure 3. SEM images of SS316L composites containing 4 wt.%Sn with 15 wt.%MoS_2 addition sintered at 1150 ºC (a) and 1200ºC (b).

The reaction between alloying elements in SS316L steel matrices and MoS_2 solid lubricant particles was observed as shown in Figure 2 (b, c, d and f, g, h). This reaction causes the formation of a liquid phase at 988 °C, according to the iron-sulfur phase diagram lead to promote densification of the 316L + MoS_2 composites samples [24]. The microstructure of SS316L + 4 wt.%Sn + 15 wt.% MoS_2 sintered at 1150 and 1200 ºC presented clearly different phases in the composites as shown in Figure 3.

Although the density of added MoS_2 powder was less than half of that of 316L stainless steel powder, the additions of MoS_2 powder insignificantly affected the density of sintered materials. The experimental results showed that the sintered density slightly decreased with respect to the increase of added MoS_2 amount (Figure 4). In the cases of sintered 316L + Sn and 316L + Sn + MoS_2 composites, the decrease of density due to the addition of lighter materials (Sn and MoS_2 powders) is compensated by enhanced densification due to LPS. Small sintered density variation with MoS_2 content was previously reported in [12, 25]. The presence of a liquid phase during sintering causes rearrangement, solution-reprecipitation and final densification as given in [26]. The liquid phase formation enhancing densification of the sintered material was also confirmed experimentally [27-28].

The chemical analysis by using EDS mapping (Figure 5), clearly showed that Cr diffused from 316L matrix to dark intergranular phases (the regions previously occupied by MoS_2 powder). Fe showed no diffusion. Sn and Ni existed at the same regions. By the comparison of Figure 3 and Figure 5, the dark intergranular phase represented mixed (Mo, Cr) sulfide whereas the bright intergranular phase represented Sn-based phase. The coexistence of Sn and Ni in sintered specimens (in this study) conforms to the Sn-based phase observed in sintered 316L + Sn alloy reported in previous work [18]. Attempt has been made to characterize phases in the sintered 17-4 PH + MoS_2 composite, whose green parts were formed by injection molding, by using X-ray diffraction (XRD) technique [17]. The interpretation of XRD peaks led to the identification of sulfides of Cr, Fe and Ni.

Although, MoS_2 can react with Fe [29] and Ni [30] to form sulfides, however, by taking the EDS mapping of element distribution (Figure 5) into account, Fe and Ni seem to have very weak

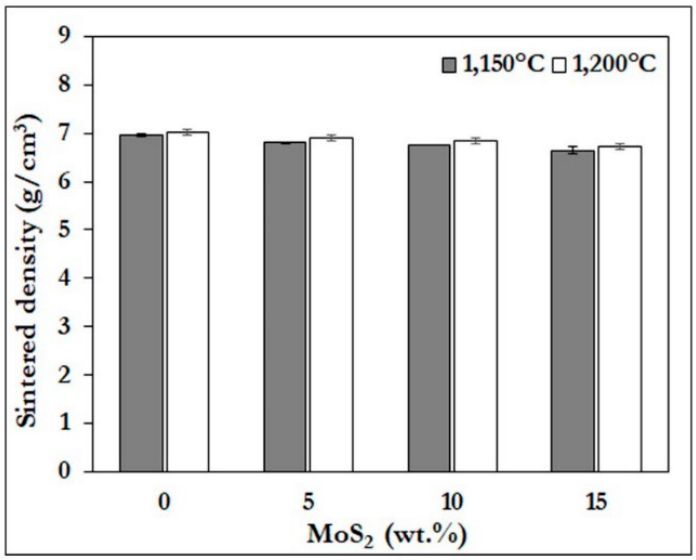

Figure 4. Sintered density of SS316L composites containing 4 wt.%Sn with variation in MoS_2 addition sintered at 1150 ºC and 1200ºC.

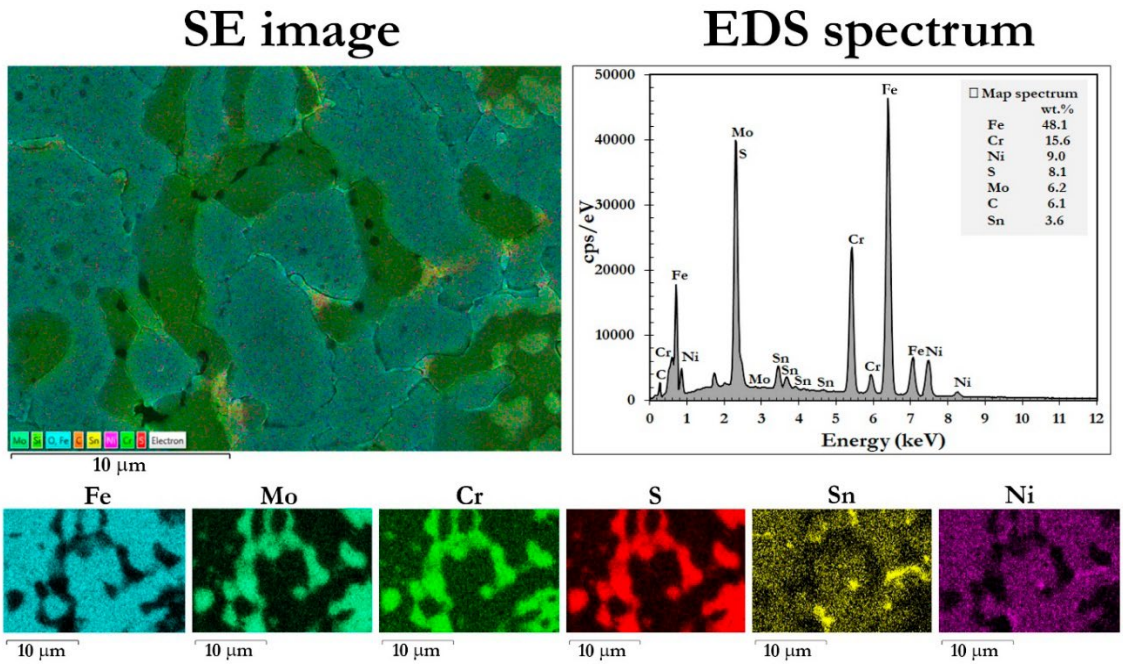

Figure 5. X-ray mapping of elements distribution in the non-eutectic-like region of SS316L composites containing 4 wt.%Sn with 15 wt.%MoS_2 addition sintered at 1150 ºC.

contribution in the dark intergranular phase whereas Ni is abundant in the bright intergranular phase. Another evidence of LPS is eutectic-like region as shown in Figure 6. The eutectic-like region consists of mixed (Mo, Cr) sulfide and unknown phase. Due to indecisive conclusion of sulfide phases, further characterization is underway.

3.2 Mechanical Properties

The mechanical properties of the sintered 316L + Sn + MoS_2 composites, including ultimate tensile strength, yield strength, elongation and hardness, were plotted against added MoS_2 amount as shown in Figure 7.

The graphs showed decreases of percentage of elongation and ultimate tensile strength with increasing MoS_2 content whereas yield strength tended to increase due to MoS_2 addition. Hardness increased with increasing MoS_2 content. According to the measured values of tensile properties given in Figure 7, the sintered 316L + Sn + MoS_2 composites have the yield strength to tensile strength (Y/T) ratio increased with increasing MoS_2 content. In addition, the difference between tensile strength and yield strength decreased with increasing MoS_2 content. The materials with high Y/T ratio and small difference between tensile strength and yield strength may be deemed as brittle materials. The low elongation values (Figure 7c) confirms brittleness of the sintered composites with high added MoS_2 content. Taking the volume fraction of thick intergranular phase into account, the intergranular phase content has direct relationship with the Y/T ratio and inverse relationship with the difference between tensile strength and yield strength.

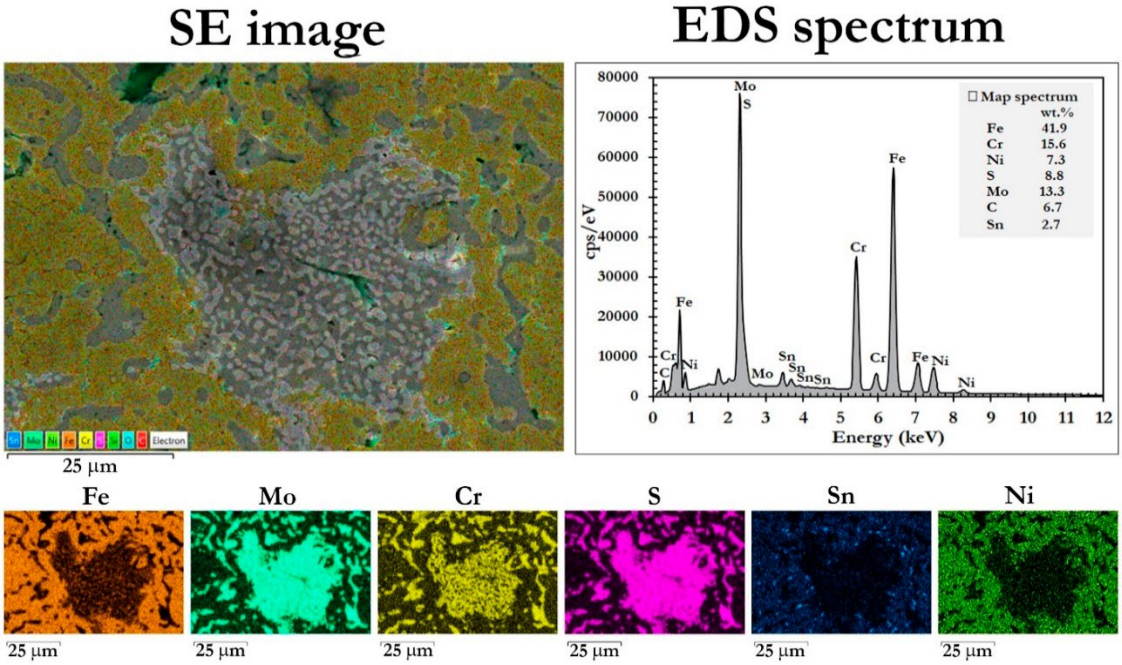

Figure 6. X-ray mapping of elements distribution in the eutectic-like region of SS316L composites containing 4 wt.%Sn with 15 wt.%MoS_2 addition sintered at 1150 ºC.

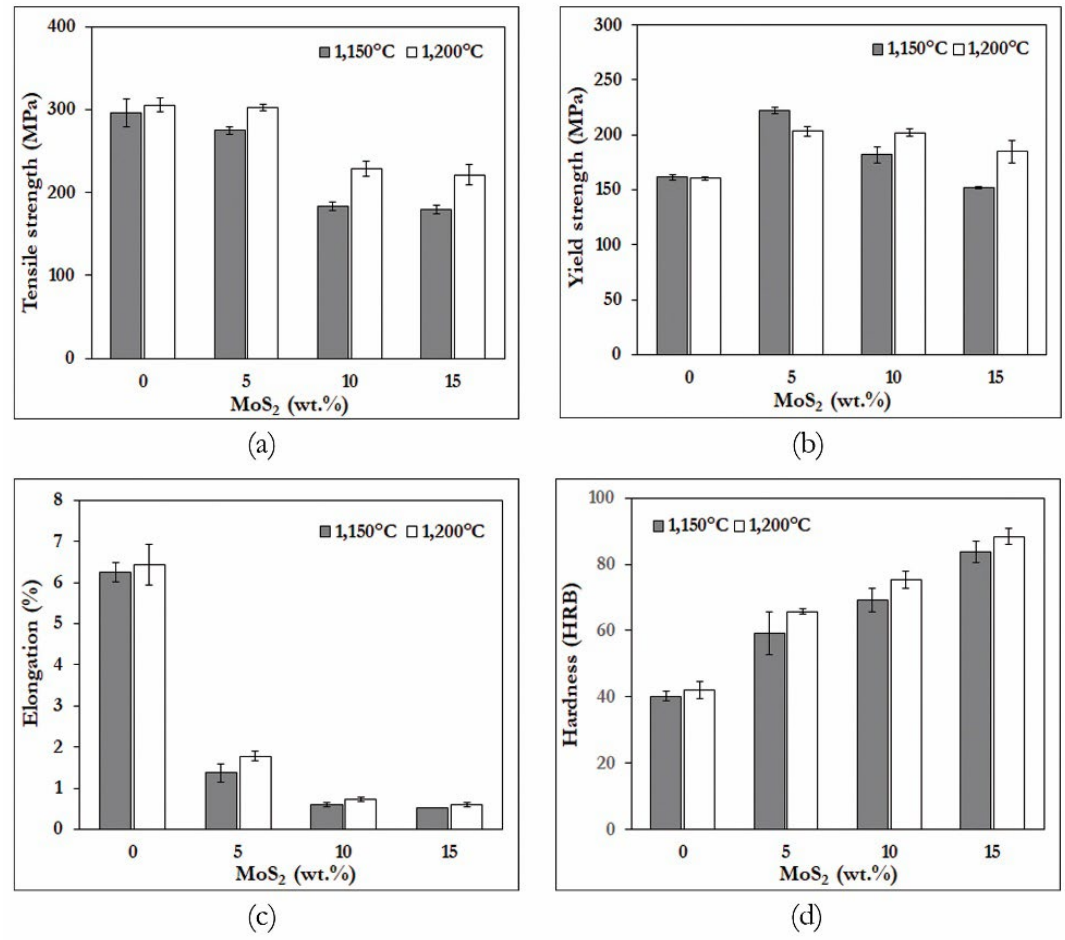

Figure 7. Mechanical properties of SS316L composites containing 4 wt.%Sn with variation in MoS_2 addition sintered at 1150 ºC and 1200ºC.

Since the measured values of tensile properties of sintered 316L + MoS_2 composites are available in previous works [12, 25], they can be compared with the respect values of sintered 316L + Sn + MoS_2 composites (this work) to clearly understand the effect of Sn addition. Tensile strengths of sintered 316L + MoS_2 composites, produced by sintering at 1300 °C, are in the ranges of 170-270 MPa [12] and 280-300 MPa [25]. Tensile strengths of sintered 316L + Sn + MoS_2 composites, produced by sintering at ≤ 1200 °C, are in the range of 180-310 MPa (this work). This comparison indicates that Sn powder addition can assist sintering even at low temperatures.

In Figure 7(c), for each alloy/composite composition elongation value of the material produced under 1200 °C sintering was higher than that of the material produced under 1150 °C sintering. The higher elongation value is due to higher sintered density (Figure 4), which is in turn attributed to high sintering temperature. In previous work, better elongation values were obtained in sintered alloys with higher sintered densities [31, 32].

3.3 Friction and Wear

The coefficient of friction (COF) of a sintered 316L + Sn + MoS_2 composite specimen was tested under the conditions given above. The measured COF values were plotted against MoS_2 amount as shown in Figure 8. Similar trends, in which COF increased slightly with increasing MoS_2 content up to 10 wt. % and after that COF dropped, were observed for both composite sets produced by sintering at 1150 and 1200 °C. In addition, the composites produced at higher sintering temperature showed higher COF values. As mentioned above, some MoS_2 powder particles decompose and react with matrix constituents to form compounds. The compound formation causes loss of MoS_2 powder particles that act as solid lubricant. In case that the reaction products do not have as good lubricating properties as MoS_2, the COF of sintered composites will also depend on surface roughness and hardness of the matrix and reaction products. The increase of bulk hardness with increasing MoS_2 content is given in Figure 7d.

The measured surface roughness values were found to be increased with increasing MoS_2 content and sintering temperature (Figure 9). The surface roughness results from different phases presenting on sintered composite surface.

The volume losses of sintered composites decreased with increasing MoS_2 content up to 10 wt. % after that it showed significantly increase as shown in Figure 10. Up to 10 wt. % MoS_2 addition, the volume loss is inversely proportional to hardness as given by Archard's equation [33]. However, the 15 wt.% MoS_2 addition caused the abrupt increase of volume loss as shown in Figure 10. This abrupt increase of volume loss may be attributed to higher volume fraction of intergranular phases as shown in Figure 2. Cracks are observed on the boundaries between matrix grains and intergranular phases (Figure 3). These cracks would ease delamination wear mechanism by enhancing the propagation of subsurface cracks at a critical depth parallel to and eventually up to the sliding surface results in the formation of flake-like debris. The material loss in the form of

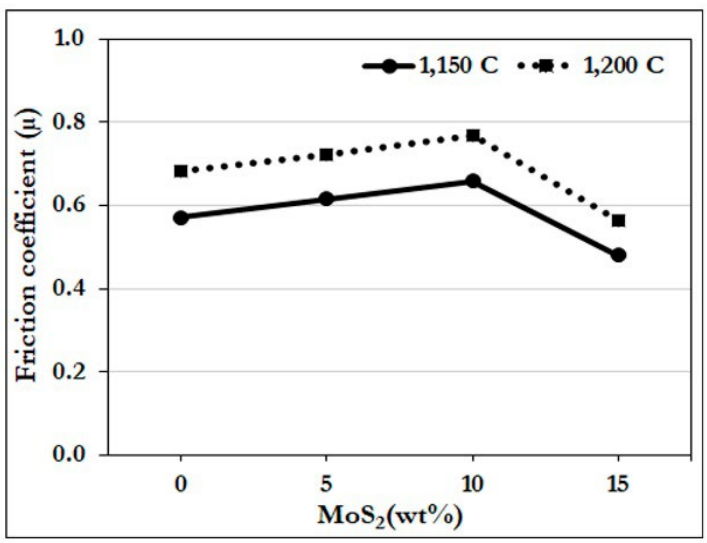

Figure 8. Friction coefficient (COF) of the SS316L composites containing 4 wt.%Sn with variation in MoS_2 addition sintered at 1150 ºC and 1200ºC.

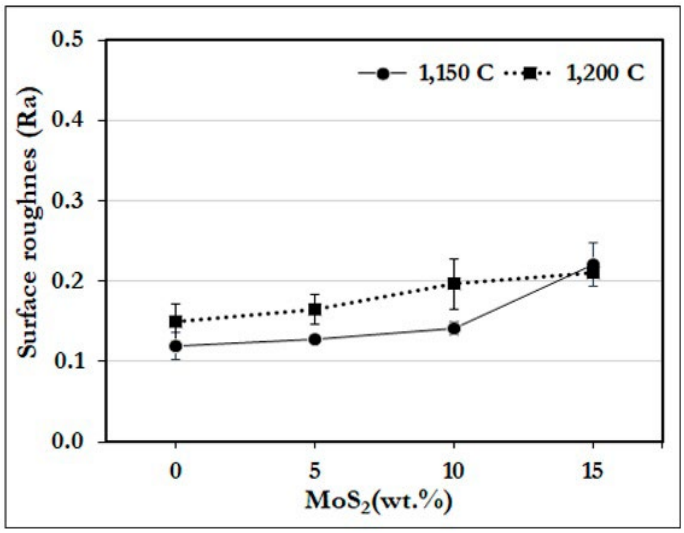

Figure 9. Surface roughness of SS316L composites containing 4 wt.%Sn with variation in MoS_2 addition sintered at 1150 ºC and 1200ºC.

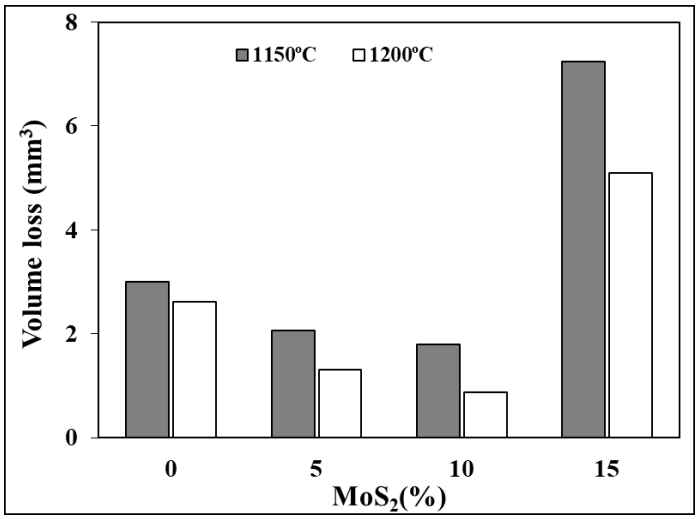

Figure 10. Volume loss of SS316L composites containing 4 wt.%Sn with variation in MoS_2 addition sintered at 1150 ºC and 1200ºC.

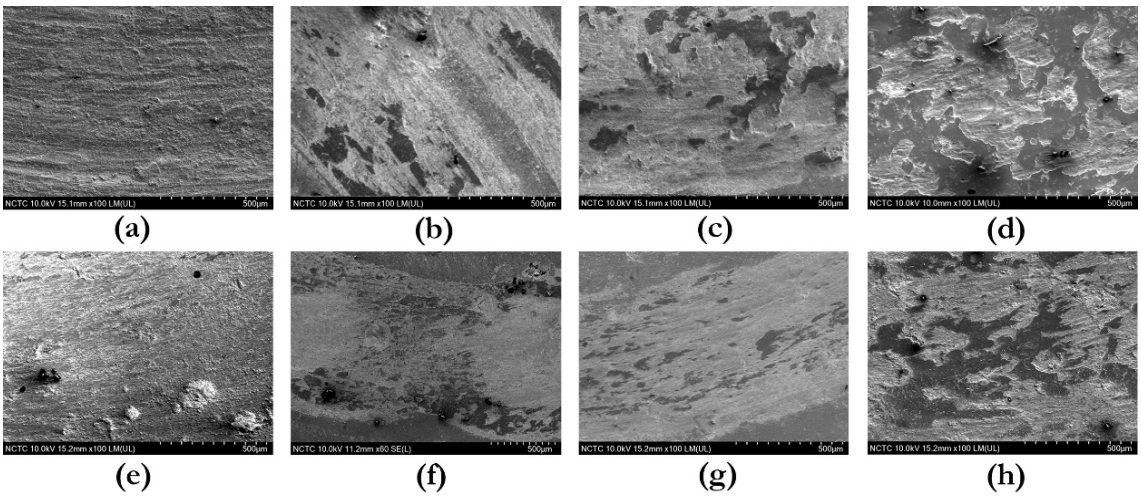

Figure 11. Worn surfaces of SS316L composites containing 4 wt.%Sn with variation in MoS_2 addition. (a) 0 wt.% MoS_2 -1150 ºC, (b) 5 wt.% MoS_2 -1150 ºC, (c) 10 wt.% MoS_2 -1150 ºC, (d) 15 wt.% MoS_2 -1150 ºC, (e) 0 wt.% MoS_2 -1200 ºC, (f) 5wt.% MoS_2 -1200 ºC, (g) 10 wt.% MoS_2 -1200 ºC and (h) 15 wt.% MoS_2 -1200 ºC.

flake-like debris in the delamination mechanism is thus related to the abrupt increase of volume loss. The worn surface was examined using FESEM, the images of them have been shown in the Figure 11(a-h). The plastic deformation, transferred materials, delamination pits, abrasive grooves and fine particles in the wear track were observed. As indicated by the worn surface wear mechanism is adhesive. The 15 wt. % MoS_2 addition specimens have the highest volume loss and high surface roughness due to the formation of large wear debris particles. Increase of MoS_2 content leads to the increasing transferred layers on the worn surface. In addition, the coverage area of transferred layer in the wear track increased corresponding to the increasing of MoS_2 content.

The presence of transferred layer on the worn surface leads to wear resistance improvement. That is why the COF of the sintered composites with 15 wt.% MoS_2 addition decreases. However, specimens produced at higher sintering temperature showed lower amount of transferred layer on the worn surface as shown in Figure 11.

It was found that the wear resistance of sintered 316L + Sn composites increased with increasing sintering temperature as shown in Figure 11(a) and Figure 11(e). High magnification SEM micrographs of worn surfaces of sintered 316L + 4 wt.% Sn + 5 wt.% MoS_2 composite revealed the evidences of adhesive, abrasive, delamination and transferred layer on the worn surface as shown in the Figure 12.

4. Conclusions

In this work, production of sintered 316L + Sn + MoS_2 composites was successful. Although sintering temperatures lower than that normally used in a conventional sintering of 316L powder compacts were used, sintered bonds could be produced. The reaction between MoS_2 solid lubricant particles and the alloying elements in 316L matrix still existed resulting in the formation of mixed sulfides dispersed in the microstructure of the sintered composites. The Sn-based phase was observed at grain boundaries, the boundaries of mixed sulfides or MoS_2 particles. Wear

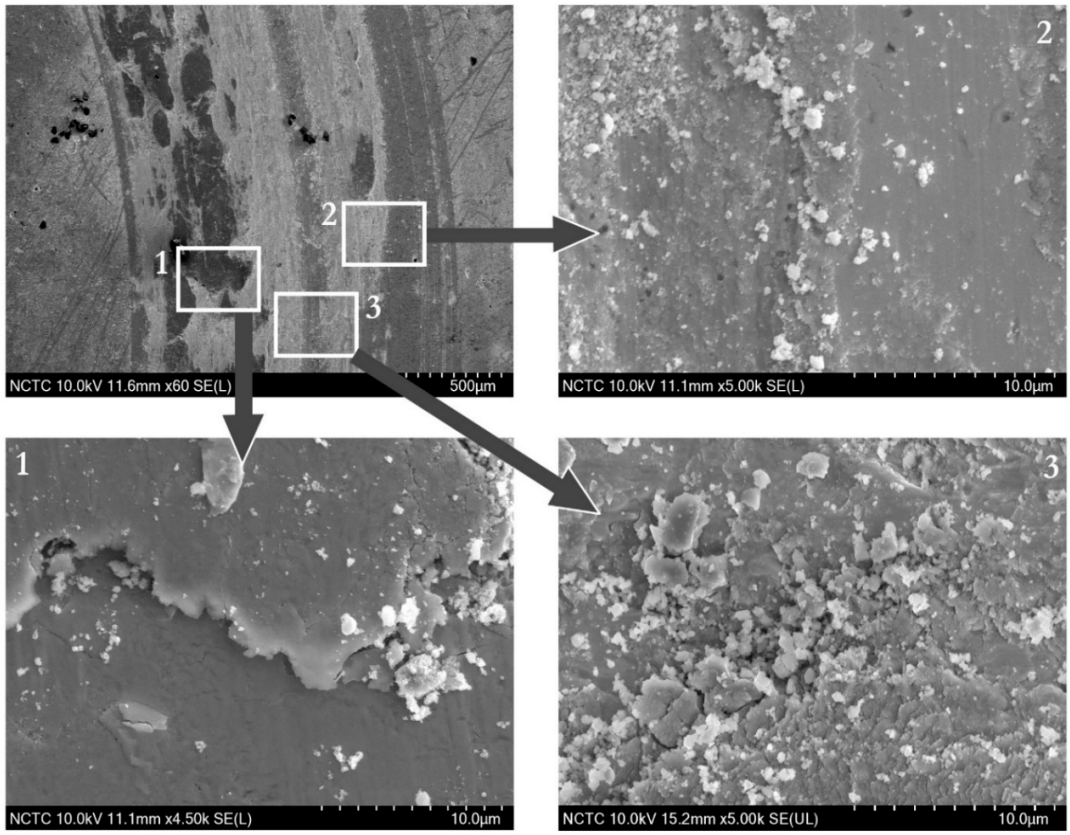

Figure 12. SEM images of worn surfaces of SS316L composites containing 4 wt.%Sn with 5 wt.%MoS_2 addition sintered at 1150 ºC.

mechanism of the sintered composites tested under dry sliding was dominated by adhesive mode. Wear resistance increased according to the MoS_2 content, however the amount of the MoS_2 content affected mechanical properties and surface roughness.

Acknowledgements

Thanks to department of Industrial Physics and Medical Instrumentation (IMI) of Faculty of Applied Science, Lasers and Optics Research Center (LANDOS) of King Mongkut's University of Technology North Bangkok, and grateful for financial supported from National Metal and Materials Technology Center (MTEC), Thailand.

References

[1] Menezes P.L., Rohatgi P.K. and Omrani E., *Self-Lubricating Composites,* Springer-Verlag GmbH, DE, Germany, 2018.

[2] Sliney H., *Solid Lubricants;* Available at: https://ntrs.nasa.gov/archive/nasa/casi.ntrs.nasa.gov/19910013083.pdf.

[3] Huang S., Feng Y., Ding K., Qian G., Liu H. and Wang Y., *Acta Metall. Sin.,* 2012; **25**: 391-400. DOI 10.11890/1006-7191-125-391.

[4] Vadiraj A., Kamaraj M. and Sreenivasan V. S., *Int. J. Innov. Res. Eng. Technol.,* 2012; **37:** 569-577.

[5] Furlan K.P., Mello J.D.B. and Aloisio N.K., *Tribol. Int.,* 2018; **120:** 280-298.

[6] Lu J., Yang S., Wang J. and Xue Q., *Wear*, 2001; **249**: 1070-1076. DOI 10.1016/S0043-1648(01)00846-8.

[7] Rapoport L., Leshchinsky V., Lvovsky M., Lapsker I., Vovolik Y., Feldman Y., Popovitz-Biro P. and Tenne R., *Wear,* 2003; **255:** 794-800. DOI 10.1016/S0043-1648(03)00285-0.

[8] Junghans R., Neukirchner J., Schumann D. and Lippman K.-H., *Tribol. Int.,* 1996; **29**: 181-192. DOI 10.1016/0301-679X(95)00087.

[9] Maslyuk V.A. and Napara-Volgina S.G., *Powder Metall. Met. Ceram.,* 1999; **38:** 521-535.

[10] Slys I.G., Perepelkin A.V. and Fedorchenko I.M., *Powder Metall. Met. Ceram.,* 1973; **12:** 710-714. DOI 10.1007/BF00793978

[11] Mahathanabodee S., Palathai T., Raadnui S., Tongsri R. and Sombatsompop N., *Wear,* 2014; **316**: 37-48. DOI 10.1016/j.wear.2014.04.015.

[12] Raadnui S., Mahathanabodee S. and Tongsri R., *Wear*, 2008; **265**: 546-553. DOI 10.1016/j.wear.2007.11.014.

[13] Furlan K.P., Patricia B.P., Thayna A.S., Matheus V.G., Heitor T.F., Batista Rodrigues N. and Aloisio N.K., *J. Alloy. Compd.*, 2015; **652**: 450-458. DOI 10.1016/j.jallcom.2015.08.242.

[14] Li L. and Xiong D.S., *Wear*, 2008; **265**: 533-539. DOI 10.1016/j.wear.2007.09.005.

[15] Slys I.G, Perepelkin A.V. and Fedorchenko I.M., Structure and properties of sintered stainless steel containing molybdenum disulfide, *Powder Metall. Met. Ceram.,* 1973; **12:** 710-714.

[16] Napara-Vologina S.G., Orlova L.N., Mamonova A.A. and Dzeganovskii V.P., *Powder Metall. Met. Ceram.,* 1997; **36(9)**: 548-553. DOI 10.1007/BF02680510.

[17] Furlan K.P., Binder C., Klein A.N. and Mello J.D.B., *J. Mater. Res. Technol.,* 2012; **1**: 134-140. DOI 10.1016/S2238-7854(12)70024-8.

[18] Tosangthum N., Piyanuch M., Coovattanachai O., Morakotjinda M., Yotkaew T., Wila P., Krataitong R., Vetayanugul B. and Tongsri R., *J. Met. Mater. Miner.,* 2008; **1**: 47-51.

[19] Sharma S.M. and Anand A., *Tribol. Ind.*, 2016; **38**: 318-331.

[20] Morakotjinda M., Fakpan K., Yotkaew T., Tosangthum N., Krataitong R., Daraphan A., Siriphol P., Wila, P., Vetayanugul B. and Tongsri R., *Chiang Mai J. Sci.,* 2010; **37**: 55-63.

[21] Coovattanachai O., Tosangthum N., Morakotjinda M., Yotkaew T., Daraphan A., Krataitong R., Vetayanugul B. and Tongsri R., *Mater. Sci. Eng. A,* 2007; **445-446**: 440-445. DOI 10.1016/j.msea.2006.09.105

[22] Tosangthum N., Coovattanachai O., Krataitong R., Morakotjinda M., Daraphan A., Vetayanugul B. and Tongsri R., *Chiang Mai J. Sci.,* 2006; **33**: 53-66.

[23] Furlan K.P., Patricia B.P., Thayna A.S., Matheus V.G., Heitor T.F., Batista R.N. and Aloisio N.K., *J. Alloy. Compd.,* 2015; **652**: 450-458. DOI 10.1016/j.jallcom.2015.08.242.

[24] Furlan K.P, Goncalves P.D.C., Binder D., Binder C. and Klein A.N., *3rd World PM 2014 - World Congress on Powder Metallurgy and Particulate Material,* Orland, USA, 18-22 May 2014.

[25] Chaiyarat N., Daopiset S., Mahathanabodee S. and Tongsri R., *Materials Today: Proceedings,* 2018; **5**: 9384-9392. DOI 10.1016/j.matpr.2017.10.114.

[26] German R.M., Suri P. and Park S.J., *J. Mater. Sci.*, 2009; **44**: 1-39. DOI 10.1007/s10853-008-3008-0.

[27] Sundaram M.V., Surreddi, K.B., Hryha E., Veiga A., Berg S., Castro F. and Nyborg L., *Metall. Mater. Trans. A*, 2018; **49**: 255-263.

[28] Johnson J.L. and German R.M., *Metall. Trans. A*, 1993; **24**: 2369-2377. DOI: 10.1007/bf02646516.

[29] Domask A.C., Gurunathan R.L. and Mohney S.E., *J. Electron. Mater.,* 2015; **44**: 4065-4079. DOI: 10.1007/s11664-015-3956-5.

[30] Parucker M.L., Klein A.N., Binder C., Junior W.R. and Binder R., *Mater. Res.,* 2014; **17**: 180-185. DOI: 10.1590/S1516-14392013005000185.

[31] Coovattanachai O., Lasutta P., Tosangthum N., Krataitong R., Morakotjinda M., Daraphan A., Vetayanugul B. and Tongsri R., *Chiang Mai J. Sci.*, 2006; **33**: 293-300.

[32] Yuan X., Qu X., Yin H., Yan Z. and Tan Z., *Materials*, 2019; **12**: 3005. DOI 10.3390/ma12183005.

[33] Patel P.J. and Patel J.M., *Int. J. Adv. Eng. Res. Dev.*, 2014; **1(2):** 2348-4470.